An Adaptive Order Godunov Type Central Scheme

Eitan Tadmor[1] and Jared Tanner[2]

[1] Department of Mathematics, Institute for Physical Science & Technology and Center for Scientific Computation And Mathematical Modeling (CSCAMM), University of Maryland College Park, MD 20742-3289 *tadmor@cscamm.umd.edu*

[2] Department of Mathematics University of California Davis, CA 95616 *jtanner@math.ucdavis.edu*

Traditionally, high order Godunov-type central schemes employ local polynomial reconstructions. These reconstructions avoid transfer of information across discontinuities through nonlinear limiters which act as local edge detectors. Here we introduce an adaptive method which employ global edge detection to ensure that information is extracted in the direction of smoothness while maintaining computational stability. Additionally, the global edge detection substantially reduces the computational cost. The reconstruction incorporates the largest symmetric stencil possible without crossing discontinuities. Consequently, the spatial order of accuracy is proportional to the number of cells to the nearest discontinuity, reaching exponential order at the interior of regions of smoothness.

1 Godunov Type Schemes

We seek an approximate solution of the hyperbolic conservation law

$$u_t + f(u)_x = 0 \qquad x \in [0, 2\pi], \quad t \geq 0. \tag{1}$$

Of particular interest are solutions with contact discontinuities, shocks, and rarefaction waves. To better handle these interesting phenomena (1) is transferred to the exact integral formulation by integrating over a control volume in space time, $[x - \Delta x/2, x + \Delta x/2] \times [t, t + \Delta t]$

$$\begin{aligned} \bar{u}(x, t + \Delta t) = \bar{u}(x, t) &- \frac{1}{\Delta x} \int_{\tau}^{\tau + \Delta t} f(u(x + \Delta x/2, \tau)) d\tau \\ &+ \frac{1}{\Delta x} \int_{\tau}^{\tau + \Delta t} f(u(x - \Delta x/2, \tau)) d\tau \end{aligned} \tag{2}$$

were $\bar{u}(x, t)$ is the spatial average of $u(x, t)$ over $[x - \Delta x/2, x + \Delta x/2]$

$$\bar{u}(x, t) := \frac{1}{\Delta x} \int_{x - \Delta x/2}^{x + \Delta x/2} u(y, t) dy. \tag{3}$$

Godunov type schemes are constructed under the integral framework, (2), which yields a relationship between the evolution of cell averages and the flux evaluations along the spatial cell boundaries.

Unlike finite difference methods which work strictly with point values Godunov methods begin with a collection of cell averages,

$$\{\bar{u}(x_j, n)\}_j \qquad x_j := (j - 1/2)\Delta x, \qquad j = 1, 2, \ldots 2\pi/\Delta x, \tag{4}$$

and form a global reconstruction, $w(x, t^n)$, to approximate $u(x, n)$,

$$w(x, t^n) := \sum_j R_j(x, t^n)\chi_{[x_j - \Delta x/2, x_j + \Delta x/2]}. \tag{5}$$

This global reconstruction is then evolved in time by relationship (2).

Two frameworks that have been used for this evolution step are the upwind and central schemes. The upwind schemes maintain the original cells for each time evolution, as a result the flux integrals in (2) are evaluated at a point of discontinuity in the global reconstruction. Consequently (approximate)Riemann solvers are needed to determine the flux integral. Although this is not a severe limitation in one dimension it complicates multidimensional calculations.

Central schemes use a staggered cell average. Given the cell averages $\{\bar{u}_j^n\}_j$ the global reconstruction is formed, (8), and from it the staggered cell averages are computed

$$\bar{w}_{j+1/2}^n := \int_{x_j}^{x_j + \Delta x/2} R_j(x, t^n)dx + \int_{x_{j+\Delta x/2}}^{x_{j+1}} R_{j+1}(x, t^n)dx. \tag{6}$$

The evolution of these staggered cell averages

$$\begin{aligned} \bar{w}_{j+1/2}^{n+1} = \bar{w}_{j+1/2}^n &- \frac{1}{\Delta x}\int_\tau^{\tau+\Delta t} f(w_{j+1}^n(x(\tau)))d\tau \\ &+ \frac{1}{\Delta x}\int_\tau^{\tau+\Delta t} f(w_j^n(x(\tau)))d\tau \end{aligned} \tag{7}$$

involves flux integrals computed at the smooth midpoints of the reconstruction, $w(x, t^n)$. This allows for the flux integrals to be calculated from quadrature formulas and consequently yields a method free of Riemann solvers. We now focus our attention on central schemes which emphasize the global reconstruction.

Extensive work has been done in determining the desired properties of such reconstructions, see [Le79, HEOC85, NT90, Sh97, LT98] and the references therein. In the original work by Godunov [Go59] a piecewise constant reconstruction was used, $w(x, t) := \sum_j \bar{u}(x_j, t)\chi_{[x_j - \Delta x/2, x_j + \Delta x/2]}$, yielding a first order upwind method. Since Godunov's original paper both upwind and central schemes have been extended to second order [Le79, NT90] and

higher. As the evolution equation is exact the overall accuracy of a scheme is dictated by the accuracy of the global reconstruction. Traditionally local polynomial reconstructions have been used,

$$w(x,t^n) := \sum_j P_j(x,t^n)\chi_j(x), \quad \chi_j := \chi_{[x_j-\Delta x/2, x_j+\Delta x/2]}, \tag{8}$$

where $P_j(x,t^n)$ is a fixed order polynomial. We now focus on the reconstruction of piecewise smooth solutions common in hyperbolic problems.

It is well known that approximations of piecewise smooth functions suffer from oscillation and poor accuracy when the approximation crosses a discontinuity. For Godunov schemes the introduction of these oscillations causes the method to be inaccurate and often times unstable. In order to avoid the introduction of oscillations methods were introduced with properties such as Total Variation Diminishing(TVD) and Number of Extrema Diminishing(NED). To satisfy these properties with more than first order accuracy the global reconstruction necessarily became nonlinear. A prototype example is provided by the minmod *limiter* for piecewise linear reconstruction

$$\begin{aligned} P_j^{mm}(x,t^n) &= \bar{u}_j^n + (x-x_j)w'(x_j,t^n) \\ w'(x_j,t^n) &:= \begin{cases} 0 & (\bar{u}_{j+1}^n - \bar{u}_j^n)(\bar{u}_j^n - \bar{u}_{j-1}^n) \le 0 \\ (\bar{u}_{j+1}^n - \bar{u}_j^n)/\Delta x & |\bar{u}_{j+1}^n - \bar{u}_j^n| \le |\bar{u}_j^n - \bar{u}_{j-1}^n| \\ (\bar{u}_j^n - \bar{u}_{j-1}^n)/\Delta x & |\bar{u}_j^n - \bar{u}_{j-1}^n| \le |\bar{u}_{j+1}^n - \bar{u}_j^n| \end{cases} \end{aligned} \tag{9}$$

This reconstruction is *limited* in the sense that which cell averages are used is determined by the local smoothness. To avoid oscillations the cell averages used are taken in the direction of greater smoothness.

Godunov's method [Go59] was extended by van Leer[Le79] who replaced the piecewise constant reconstruction by (9) yielding a second order upwind method. As with the piecewise constant reconstruction the minmod reconstruction satisfies the three properties

1. Conservation — the reconstruction retains the same average

$$\frac{1}{\Delta x}\int_{x_j-\Delta x/2}^{x_j+\Delta x/2} P_j^{mm}(x,t^n) \equiv \bar{u}_j^n \tag{10}$$

2. Non-Oscillatory — furnished for example, by the TVD property $\|\sum P_j(\cdot,t^n)\chi_j(x)\|_{BV} \le \|\sum \bar{u}_j\chi_j(\cdot)\|_{BV}$.
3. Accuracy — a finite polynomial accuracy

$$|P_j(x,t^n) - u(x,t^n)| \le O(h^r), \;\; r \text{ fixed} \;\; x \in \left[x_j - \frac{\Delta x}{2}, x_j + \frac{\Delta x}{2}\right]. \tag{11}$$

The second order accuracy of (9) can be increased by using higher order polynomial reconstructions where care is taken not to introduce oscillations.

Direct extensions can be found in [Sh97, LT98]... As with (9), limiters are applied so that the stencil changes in the direction of smoothness and spurious oscillations are avoided (or at least, significantly reduced).

The nonlinear limiters used in these polynomial reconstructions can be seen as *local edge detectors*, as they encourage the reconstruction to use information which does not cross a discontinuity. In the context of the Weakly Non-Oscillatory (WENO) reconstructions, [LPR99], the limiters are referred to as "smoothness indicators". As each cell recomputes the smoothness indicators, the action of these local edge detectors is redundant, consult e.g., [LPR99, Pu02]. Indeed, though solutions of (1) are sought within the class of BV functions. In actual simulations, however, these solutions are realized as piecewise smooth solutions, where finitely many jumps separate between regions of smoothness, [Ta02]. It is therefore makes sense to adopt a global point of view: to use a global sweep to detect *all* edges and to reconstruct highly accurate polynomials in between those edges.

In the next section we use the adaptive mollifier of [TT02] yielding a symmetric reconstruction of order proportional to the number of cells to the nearest discontinuity. Unlike the traditional local finite-order polynomial reconstructions, the present stencils are not restricted to a fixed size; instead, the usage of the whole region of smoothness enables us to achieve higher – in fact exponential accuracy.

2 An adaptive order central scheme

Below we construct a central scheme with explicit global edge detection and an adaptive order symmetric reconstruction. The global edge detector is more efficient than the polynomial limiters as it locates all discontinuities at once. Once these locations are known we form a global reconstruction with accuracy proportional to the number of cells to the nearest discontinuity. We conclude by investigating this schemes treatment of contact discontinuities, shocks and rarefaction waves in scalar advection equations.

2.1 Global Edge Detection

Accurate reconstructions of piecewise smooth data require the discontinuity locations. In [GeTa99, GeTa00b] Gelb and Tadmor analyzed and constructed a family of *global* edge detectors which use a function's (pseudo)spectral information. For our Godunov type scheme we used the exponential concentration kernel introduced in [GeTa00b]

$$K_N^\sigma(t) := -\sum_{k=1}^{N} \sigma(\frac{k}{N}) \sin kt \quad \sigma(\eta) := Const.\eta e^{1/\eta(\eta-1)}. \tag{12}$$

Under proper normalization convolving the concentration kernel with the spectral projection, $K_N^\sigma \star S_N f(x)$, converges to the jump function $[f](x) := f(x^+) - f(x^-)$. Automated use of edge detection for the reconstruction method requires a simple indication whether a particular cell contain a discontinuity. This can be achieved by a new procedure for separation of scales advocated in [GeTa02]. Here, one implement a minmod limiter, $\text{minmod}(K_N^\sigma \star S_N f(x_j), f(x_{j+1}) - f(x_{j-1})$ followed by a simple thresholding of order $\Delta x \max |f(x)|$.

2.2 Adaptive Order Reconstruction

Spectral projections of smooth functions posses exponential convergence; however the presence of a single jump discontinuity reduces the convergence to at most first order. In [GoTa85] Gottlieb and Tadmor developed a two parameter, (p, θ) mollifier, composed of a smooth localization function ρ_c and the Dirichlet kernel of order p

$$\psi_{p,\theta}(x) := \frac{1}{\theta}\rho_c(\frac{x}{\theta})D_p(\frac{x}{\theta}), \quad \rho_c := e^{\left(\frac{cx^2}{x^2-\pi^2}\right)}, \ c > 0. \tag{13}$$

This mollifier recovers the exponential convergence for (pseudo)spectral projections of *piecewise* smooth data. In [TT02] by further analyzing (13) we determined the optimal parameters to be *adaptive*, depending on the distance to the nearest discontinuity, namely

$$\begin{aligned} &\theta = \theta(x) := \frac{d(x)}{\pi}, \quad d(x) = dist(x, sing\ supp f) \\ &p = p(x) \sim \kappa \cdot \theta(x) N, \quad 0 < \kappa = \beta \log \beta < 1. \end{aligned} \tag{14}$$

Of particular interest for our Godunov type scheme is the manipulation of the equidistant sampling of piecewise smooth. The corresponding result from [TT02] is the error bound for the adaptive mollifier where the two parameters are given by (14) with $\kappa = 1$,

$$\left| \frac{\pi}{N} \sum_{\nu=0}^{2N-1} \psi_{p,\theta}(x - y_\nu) f(y_\nu) - f(x) \right| \le Const_c \cdot (d(x)N)^2 \left(\frac{\beta}{e}\right)^{2\sqrt{\beta \eta_c \theta(x) N}}. \tag{15}$$

When normalized to have unit mass the adaptive mollifier possesses first order accuracy in the $O(1/N)$ neighborhood of discontinuities and exponential accuracy away. It should also be noted that this mollifier can be used to compute derivatives from equidistant stencils. The derivative of the mollifier applied to the data converges to the derivative of the data with exponential accuracy similar to (15).

Using the adaptive mollifier as a tool for the reconstruction step in our Godunov type scheme results in an adaptive order proportional to the number of cells to the nearest discontinuity.

2.3 The numerical scheme

Godunov schemes that are second order and higher involve local edge detection through the use of nonlinear limiters and smoothness indicators. This implicit edge detection is used to form polynomial reconstructions of finite order. In section 2.1 we discussed the global edge detection which utilize the distance function, $d(x)$ dictated in the adaptive mollifier (13). Using these tools we form a semi-global central scheme with accuracy proportional to the number of cells to the nearest discontinuity.

The adaptive order reconstruction begins by forming the primitive of $w(x,t^n)$ from the given cell averages, (4),

$$W(x_j,t^n) := \sum_{k=0}^{j} \bar{w}_j^n \equiv \int_0^{x_j+\Delta x/2} w(x,t^n)dx \tag{16}$$

This converts the cell averages into pointvalues of the primitive. The global reconstruction is then formed by adaptive differentiation of the primitive

$$w(x,t^n) := -\frac{\pi}{N}\sum_{j=0}^{2N-1} W(y_j,t^n)\frac{d}{dx}\psi_{Nd(x)-1}(x-y_j) \qquad d(x) \geq m\Delta x. \tag{17}$$

To limit oscillations in the immediate vicinity of the discontinuities, $d(x) < m\Delta x$, a fixed number, say m neighboring cells are treated with a local, user defined polynomial reconstructions such as those in [NT90, LT98].

The staggered cell averages are computed by "integrating" the reconstruction (17) which corresponds to a divided difference of the primitive midpoints

$$W(x_j-\Delta x/2,t^n) \sim \sum_{j=0}^{2N-1} W(y_j,t^n)\psi_{Nd(x)}\left(x_j-\frac{\Delta x}{2}-y_j\right) \qquad d(x) \geq m\Delta x. \tag{18}$$

For the fixed number of cells near discontinuities, $d(x) < m\Delta x$, the primitive midpoints can be calculated by adding the exact integration of the polynomial reconstruction to the nearest primitive value to the left. The staggered cell averages are then computed by

$$\bar{w}_{j+1/2}^n := \frac{1}{\Delta x}(W(x_j+\Delta x/2,t^n) - (W(x_j-\Delta x/2,t^n)). \tag{19}$$

We note that $w(\cdot,t^n)$ is not an exact interpolant of $W(\cdot,t^n)$. Consequently, the conservation property, (10), is satisfied modulo the exponentially small and hence negligible error (15).

3 Numerical Experiments

To examine the accuracy of our adaptive order method we compute approximate solutions to two prototypical problems, linear advection and Burgers'

equation. In these problems we focus our attention on the local accuracy and the evolution of the largest errors. This is of paramount importance to determine if the low order regions pollute the overall accuracy.

At each step Godunov type schemes project the approximate solution into cell averages. The approximate cell averages can be decomposed into the true average and the local error, $\bar{w}_j^n = \bar{u}_j^n + e_j^n$. The evolution of the approximate solution (7) can be viewed as evolving both the exact solution and the local error. As the evaluation step propagates the exact solution along its characteristics part of the local error must similarly follow. The most that can be hoped for in our adaptive order method is that the error does not spread from low order regions near discontinuities to the smooth regions.

In the following examples we examine how our adaptive central scheme treats the three primary phenomena of scalar hyperbolic conservation laws; contact discontinuities, shocks, and rarefaction waves. In all cases $\Delta x := \pi/N$ and $\Delta t \sim \Delta x$. Near discontinuities, $d(x) \leq 2\Delta x$, the global reconstruction, (17), reduces to the piecewise linear reconstruction (9) and consequently to the NT scheme [NT90].

We begin our examination of discontinuities by computing an approximate solution to the linear advection equation, $u_t + u_x = 0$, with periodic boundary conditions. The initial condition $u(x,0) = f(x)$,

$$f(x) = \begin{cases} \sin(x/2) & x \in [0,\pi) \\ -\sin(x/2) & x \in [\pi, 2\pi) \end{cases} \qquad (20)$$

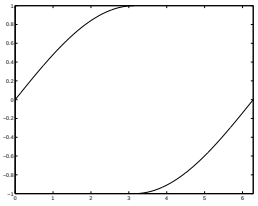

has a discontinuity at $x = \pi$ which is advocated to $x = \pi + 2$. In figure 1(b) we see that the initial error committed at $x = \pi$ is advected with the discontinuity leaving high order accuracy in the smooth region, including the path of the discontinuity. Observe the local $l_1[\frac{7}{8}\pi, \frac{9}{8}\pi]$ error in table 1. Slight blurring about the contact discontinuity can be seen in figure 1(a). This can be reduced by increasing the local polynomial reconstruction from second order [NT90] to third [LT98].

To examine a moving shock we turn to the non-linear periodic Burgers' Equation,

$$u_t + \left(\frac{u^2}{2}\right)_x = 0, \qquad (21)$$

with periodic initial conditions $u(x,0) = 1 + f(x)$, (20). As in the case of the contact discontinuity, the initial discontinuity at $x = \pi$ is advected to $x = \pi + 2$ without contaminating the regions it moves through, see figure 2(b) and table 2. In fact, the self focusing helps to narrow the low order region surrounding the discontinuity.

The final phenomena we examine is rarefaction waves. We again examine the periodic Burgers' equation but with initial conditions $u(x,0) = -f(x)$, (20), evolved to the final time $T = 1$. In this case the initial discontinuity at $x = \pi$, opens to a linear entropy solution in $[\pi - 1, \pi + 1]$, see figure 3(a). The characteristics used to fill this domain originate from the initially low order region, $x = \pi$, and consequently the fan's region also suffers from low order accuracy, figure 3(b). As for the linear advection equation the low order accuracy does not flow against the characteristics and hence leaves high resolution in the rest of the domain.

Table 1. Error measurements for figure 1(b), $\Delta x = \pi/N$, $\Delta t = \Delta x/2$. The flux evaluations were evaluated with Simpson's quadrature were the necessary midpoints were computed using the traditional RK4.

N	$l_1[0, 2\pi]$	Rate (2^{-x})	Ave $\log_{10}(error)$	$l_1[\frac{7}{8}\pi, \frac{9}{8}\pi]$	Rate (2^{-x})
40	0.351	0.97	-3.86	8.55×10^{-6}	6.86
80	0.179	0.64	-5.59	7.38×10^{-8}	5.63
160	0.115		-6.78	1.49×10^{-9}	

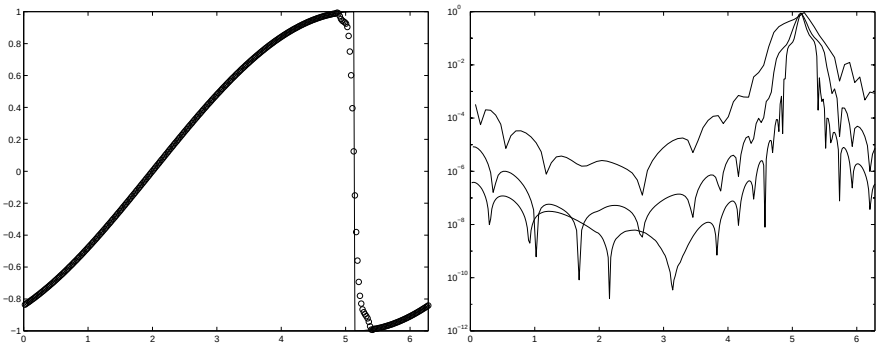

(a) (b)

Fig. 1. Approximate solution(circle) and exact solution(line) of the periodic linear advection equation at $T = 2$ with $N = 160$ (a) and the $\log_{10}$(error) for $N = 40, 80, 160$, (b).

Table 2. Error measurements for figure 2(b), $\Delta x = \pi/N$, $\Delta t = \Delta x/4$. Flux evaluations as per table 1.

N	$l_1[0, 2\pi]$	Rate (2^{-x})	Ave $\log_{10}(error)$	$l_1[\frac{7}{8}\pi, \frac{9}{8}\pi]$	Rate (2^{-x})
40	0.097	0.96	-4.39	2.09×10^{-6}	6.76
80	0.050	1.25	-6.14	1.93×10^{-8}	6.84
160	0.021		-7.97	1.69×10^{-10}	

To summarize, accuracy at a given point is determined by the accuracy used to compute points along its analytical domain of dependence. Very high order is achieved in the trails of contact discontinuities and shocks. the accuracy deteriorates, however, with low order boundary calculations and inside rarefaction fans and future work is required to study the latter.

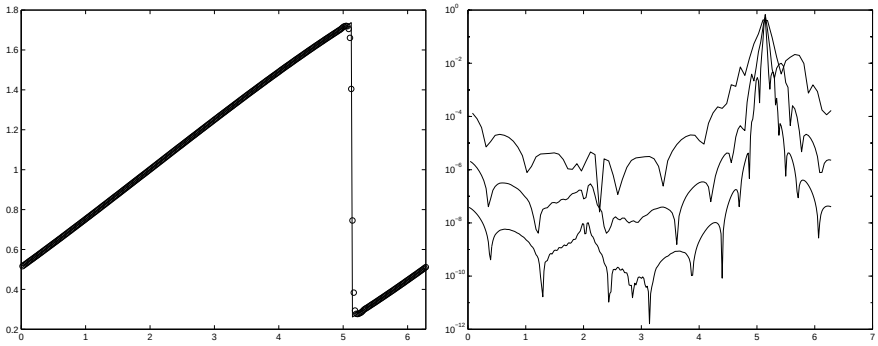

(a) (b)

Fig. 2. Approximate solution(circle) and exact solution(line) for Burgers' equation at $T = 2$, $N = 160$ (a) and the $\log_{10}$(error) for $N = 40, 80, 160$, (b).

Table 3. Error measurements for figure 3(b), $\Delta x = \pi/N$, $\Delta t = \Delta x/2$. Flux evaluations as per table 1.

N	$l_1[0, 2\pi]$	Rate (2^{-x})	Ave $\log_{10}(error)$	$l_1[\frac{7}{8}\pi, \frac{9}{8}\pi]$	Rate (2^{-x})
80	0.055	1.33	-4.13	9.83×10^{-3}	2.02
160	0.022	1.07	-5.37	2.43×10^{-3}	0.86
320	0.010		-6.55	1.34×10^{-3}	

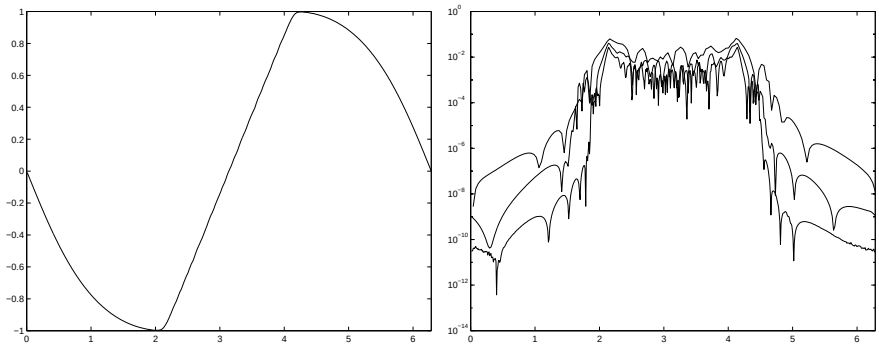

(a) (b)

Fig. 3. Approximate solution for Burgers' equation at $T = 2$ with $N = 320$ (a) and $\log_{10}$(error) for $N = 80, 160, 320$, (b).

References

[Ge00] A. Gelb, *A Hybrid Approach to Spectral Reconstruction of Piecewise Smooth Functions*, Journal of Scientific Computing, October 2000.

[GeTa99] A. Gelb and E. Tadmor, *Detection of Edges in Spectral Data*, Applied Computational Harmonic Analysis 7, (1999) 101-135.

[GeTa00b] A. Gelb and E. Tadmor, *Detection of Edges in Spectral Data II. Nonlinear Enhancement*,SIAM Journal of Numerical Analysis, 38 (2000), 1389-1408.

[GeTa02] A Gelb and E. Tadmor, *An Adaptive Edge Detection Method for Piecewise Smooth Functions*, in preparation.

[Go59] S.K. Godunov, *A finite difference method for the numerical computation of discontinuous solutions of the equations of fluid dynamics.*, Mat. Sb, 47 (1959), 271-290.

[GoTa85] D. Gottlieb and E. Tadmor, *Recovering pointwise values of discontinuous data within spectral accuracy*, in "Progress and Supercomputing in Computational Fluid Dynamics", Proceedings of 1984 U.S.-Israel Workshop, Progress in Scientific Computing, Vol. 6 (E. M. Murman and S. S. Abarbanel, eds.). Birkhauser, Boston, 1985, 357-375.

[HEOC85] A. Harten, B. Engquist, S. Osher and S.R. Chakravarthy, *Uniformly high order accurate essentially non-oscillatory schemes. III*, Jour. Comput. Phys. 71, 1982, 231-303.

[Le79] B. van Leer, *Towards the ultimate conservative difference scheme, V. A second order sequel to Godunov's method.* JCP 32 (1979), 101-136.

[LPR99] D. Levy, G. Puppo, and G. Russo, *Central WENO schemes for hyperbolic systems of conservation laws.* Math. Mod. and Numerical Analysis (1999), 547-571.

[LT98] X.D. Liu and E. Tadmor, *Third order nonoscillatory central scheme for hyperbolic conservation laws.* Numer. Math. 79 (1998), 397-425.

[NT90] H. Nessyahu and E. Tadmor, *Non-oscillatory central differencing for hyperbolic conservation laws.* JCP 87 (1990), 408-448.

[Pu02] G. Puppo, *Adaptive application of characteristic projection for central schemes*, preprint.

[Sh97] C.-W. Shu, *Essentially non oscillatory and weighted essentially non oscillatory schemes for hyperbolic conservation laws*, in "Advanced Numerical Approximation of Nonlinear Hyperbolic Equations" (A. Quarteroni, ed), Lecture Notes in Mathematics #1697, Cetraro, Italy, 1997.

[Ta94] E. Tadmor, *Spectral Methods for Hyperbolic Problems*, from "Lecture Notes Delivered at Ecole Des Ondes", January 24-28, 1994. Available at http://www.math.umd.edu/~tadmor/pub/spectral-approximations/Tadmor.INRIA-94.pdf

[Ta02] E. Tadmor, *High Resolution Methods for Time Dependent Problems with Piecewise Smooth Solutions*, "International Congress of Mathematicians" Proceedings of ICM02 Beijing 2002 (Li Tatsien, ed.), Vol.III: Invited Lectures, Higher Education Press, 2002, pp. 747-757.

[TT02] E. Tadmor and J. Tanner, *Adaptive Mollifiers - High Resolution Recovery of Piecewise Smooth Data from its Spectral Information*, J. Foundations of Comp. Math. 2 (2002), 155-189.